

Mode-coupling approach to polymer diffusion in an unentangled melt. II. The effect of viscoelastic hydrodynamic interactions

J. Farago, H. Meyer, J. Baschnagel, and A. N. Semenov

Institut Charles Sadron, Université de Strasbourg, CNRS UPR22, 23 rue du Loess, 67034 Strasbourg Cedex 2, France

(Received 6 June 2011; published 25 May 2012)

A mode-coupling theory (MCT) version (called hMCT thereafter) of a recently presented theory [Farago, Meyer, and Semenov, *Phys. Rev. Lett.* **107**, 178301 (2011)] is developed to describe the diffusional properties of a tagged polymer in a melt. The hMCT accounts for the effect of viscoelastic hydrodynamic interactions (VHIs), that is, a physical mechanism distinct from the density-based MCT (dMCT) described in the first paper of this series. The two versions of the MCT yield two different contributions to the asymptotic behavior of the center-of-mass velocity autocorrelation function (c.m. VAF). We show that in most cases the VHI mechanism is dominant; for long chains and prediffusive times it yields a *negative* tail $\propto -N^{-1/2}t^{-3/2}$ for the c.m. VAF. The case of non-momentum-conserving dynamics (Langevin or Monte Carlo) is discussed as well. It generally displays a distinctive behavior with two successive relaxation stages: first $-N^{-1}t^{-5/4}$ (as in the dMCT approach), then $-N^{-1/2}t^{-3/2}$. Both the amplitude and the duration of the first $t^{-5/4}$ stage crucially depend on the Langevin friction parameter γ . All results are also relevant for the early time regime of entangled melts. These slow relaxations of the c.m. VAF, thus account for the anomalous subdiffusive regime of the c.m. mean square displacement widely observed in numerical and experimental works.

DOI: [10.1103/PhysRevE.85.051807](https://doi.org/10.1103/PhysRevE.85.051807)

PACS number(s): 83.80.Sg, 47.57.Ng, 66.20.Cy

I. INTRODUCTION

It is commonly accepted that the dynamics of polymer chains in unentangled melts is well described by the classical Rouse model [1,2], a single-chain theoretical approach assuming Fickian diffusion dynamics of the monomers and neglecting excluded-volume interactions of chain segments. However, recent experimental and computer simulation studies [3,4] show that certain dynamical phenomena in unentangled polymer melts cannot be explained within the Rouse paradigm. One of the puzzling observations is the anomalous diffusion of the center-of-mass (c.m.) of a polymer chain at pre-Rouse times $t < t_N$, where $t_N \propto N^2$ is the Rouse relaxation time of a polymer coil of N monomer units (see Refs. [3–9] and the introduction in the preceding paper [10] of this series).

The anomalous c.m. diffusion and previous attempts to explain it are analyzed in part I, where we developed a density-based mode-coupling theory (dMCT) [10]. This approach yields a partial success: While the dMCT accounts for the observed anomalous time dependence ($t^{-5/4}$ tail) of the c.m. velocity autocorrelation function (c.m. VAF) of systems thermalized with a Langevin or Monte Carlo dynamics, the theory seems to strongly underestimate the magnitude of the effect.

Nevertheless, we are confident that the dMCT of Ref. [10] describes correctly the physical features implicitly assumed by the choice of the so-called relevant decay channel in the memory kernel. This statement may seem to be surprising, since normally it is difficult to draw a definite conclusion concerning the quantitative validity of a MCT. However, in the present case we are assisted by the fact that another approach, based on the general theory of near-equilibrium dissipative systems and outlined in Appendix B of part I [10], yields results identical to the dMCT. Moreover, the validity of this dynamic perturbation theory approach can be assessed more easily (we neglect inertial effects in this discussion for simplicity): Apart from the fluctuation-dissipation theorem (FDT) and

time-reversal symmetry arguments (both of which are rigorous), the approach hinges on the following approximations: (1) The velocity of a polymer segment is proportional to the molecular force f acting on it; (2) the force f can be represented as a sum of a regular force f_n defined by the coarse-grained molecular field conjugate to density and the random white noise ψ : $f = f_n + \psi$; (3) the molecular force f_n is assumed to act only perturbatively on the single-chain properties. The third assumption is fully justified by the strong overlap of polymer coils in the melt state (a large number of mutually overlapping chains) leading to nearly Gaussian chain size (the Flory theorem) and nearly Rousean chain relaxation time, with a small correction $\propto 1/\sqrt{N}$ (see Ref. [10]; the relative correction is proportional to $1/\sqrt{g}$ for a blob of g monomers). The second assumption reflects the standard physical separation of variables into two groups (corresponding to f_n and ψ): slow low- q components of the density field (with length scales $1/q \gg b$, where b is the monomer size) and fast high- q fluctuations of the molecular field (on microscopic length scales providing relaxations of monomer momenta) leading to Markovian dynamics of the whole system configuration. As for the first assumption, it is justified, but only partially, by the weakness of the inertial effects and by the absence of topological constraints (the chain segments can cross each other). To strictly ensure the validity of the first hypothesis we have to modify the physical model by introducing an artificial quiescent medium (thermostat) providing a friction force $-\zeta_1 v$ on each monomer moving with *absolute* velocity v . (Note that the white noise fluctuation force like $\psi(t)$, which is responsible for partial stochasticization of monomeric motion, always comes, according to the FDT, together with its dissipative counterpart, the friction force f_{fr} ; however, the direct relation of f_{fr} with the *absolute* velocity is an *assumption*, albeit a standard one.) Therefore, we may question the assumption (1) as such a thermostat is normally not present in reality.

Indeed, in real polymer melts the friction force on a monomer results from the *difference* of its velocity with respect to that of the surrounding polymer matrix, which can itself be in motion (in other words, it is a function of the *relative* velocity of the monomer with respect to the local hydrodynamic velocity field only). Such a collective continuous (“hydrodynamic”) flow of the polymer matrix was totally neglected in the preceding part I [10] and in all other theoretical studies on anomalous c.m. diffusion in melts. As we show in this paper, the collective flow effect is very important: It provides the dominant contribution to the anomalous pre-Rouse c.m. dynamics (while the effect of density fluctuations analyzed by the dMCT can be neglected in most cases).

To this end, we devise a new version of the MCT taking into account the collective flow (hydrodynamic interactions) effects and we refer to it as hMCT below. An equivalent alternative approach based entirely on the concept of hydrodynamic interactions, appropriately generalized to take into account viscoelastic hydrodynamic effects inherent in polymer melts, has been developed and briefly described in Ref. [11]. Still another derivation using a fluctuating hydrodynamics approach is given in Ref. [12].

The newly proposed hMCT mechanism (based on the coupling of the c.m. velocity to the hydrodynamic flow) is studied in Sec. II. As in Ref. [10], we focus on the c.m. VAF, $C_{c.m.}(t) = \langle V_x(0)V_x(t) \rangle$ (V_x is the x component of the c.m. velocity of the tagged chain), rather than the mean-square displacement (MSD) of the c.m. of a tagged chain, $h_{c.m.}(t) = \frac{1}{6} \langle [R_{c.m.}(t) - R_{c.m.}(0)]^2 \rangle$ [$R_{c.m.}(t)$ is the c.m. position of a tagged chain]. The two quantities are closely related [$C_{c.m.}(t) = \ddot{h}_{c.m.}(t)$], but the anomalous effect in $C_{c.m.}$ is much more visible due to the absence of the Fickian diffusion contribution. We first review (Sec. II A) the existing MCT theory for the hydrodynamic coupling in *simple fluids*, which accounts for long-time tails $\propto t^{-3/2}$ in the VAF. As an interesting intermediate example of hydrodynamic coupling, we study the c.m. VAF of a single polymer in a Θ solvent in Sec. II B. In particular, we show that the hMCT predicts a diffusion coefficient proportional to $N^{-1/2}$, in accordance with the Zimm theory, and a two-step relaxation of the VAF, a fact which is then analyzed in terms of the polymer scaling theory. This section precedes the hMCT study of the c.m. motion in a melt (Sec. II C), where the hydrodynamic interactions are intermingled with a viscoelastic response. We show that the resulting viscoelastic hydrodynamic interactions (VHIs) lead to a power law tail proportional to $-N^{-1/2}t^{-3/2}$ of the c.m. VAF for pre-diffusive times. This VHI effect largely dominates over the correlation hole effect (described by the dMCT) as long as the microscopic dynamics conserves the total momentum.

Then, we also study (Sec. III) the widespread situation of a melt driven by non-momentum-conserving dynamics (like in numerical simulations under Monte Carlo or Langevin dynamics) and show that the loss of the conservation law modifies the velocity relaxation of the c.m., although the VHIs still make a strong contribution to the c.m. motion. We also discuss the special case of Monte Carlo simulations [13], where the actual monomeric friction may be so high that the dMCT-predicted regime ($-N^{-1}t^{-5/4}$) for the c.m. VAF could

be recovered, reflecting a weighed combination of correlation hole and VHI effects.

II. HYDRODYNAMIC RELAXATION MODE-COUPLING THEORY

The dMCT for simple fluids, as sketched in Ref. [10], is relevant for situations where the density is high enough to substantiate the concept of a steric cage from which the particle must “escape” to enter the diffusion regime (the term “escape” does not account perfectly for the actual scenario; one should rather speak of a concerted dissolution of the cage). For intermediate densities, this physical picture is no longer valid, as testified by the absence of negative correlations in the VAF at these densities [14]. On the contrary, the prominent physical feature of this regime is an efficient coupling of the velocity of the tagged particle to the hydrodynamic flow of the surrounding molecules, leading to the well-known positive long-time tails and a noticeable increase of the diffusion coefficient with respect to the Enskog value [15–20]. An alternative mode-coupling approach has been devised to account for such long-time tails in the VAF [21], and this MCT (termed hMCT hereafter) is briefly described in the following section. We see that quite unexpectedly, this version of the mode-coupling theory is also relevant to describe the anomalous subdiffusive regime of the c.m. diffusion of *dense* melts, for both momentum-conserving *as well as dissipative* dynamics.

A. Simple fluids at intermediate densities

Since the seminal work by Alder and Wainwright [16], it is well known that the decay of the VAF in a fluid at intermediate densities displays a so-called long-time power law tail with an exponent $-3/2$ in three dimensions. It was soon been recognized by many authors (see [14] and references therein) that this positive long-time tail reflects the coupling of the initial velocity fluctuation of the tagged particle to the global hydrodynamic flow: The rotational part of the initial velocity field fluctuation diffuses with a diffusion coefficient $\nu = \eta/(nm)$ (η is the dynamic shear viscosity, n the number density of molecules, m the mass of a molecule). By conservation of momentum, this imposes the long-time tail $\propto t^{-3/2}$ for the tagged particle velocity relaxation [21]. The mode-coupling implementation of this physical picture works as follows: One makes explicit the hydrodynamic coupling between the tagged velocity and the hydrodynamic flow by projecting out the tagged velocity over the set of bilinear variables $C_{\alpha,k} = e^{-ik \cdot r} j_{\alpha}(k)$, where r is the position of the tagged particle and $j_{\alpha}(k) = \sum_{j=1}^{N_0} v_{\alpha,j} \exp(ik \cdot r_j)$ is the α th component of the microscopic velocity field (k is the wave vector, the sum extends over all N_0 particles of the fluid). This MCT approach leads to the following prediction of the particle VAF $C_0(t) = \langle v_x(0)v_x(t) \rangle$:

$$C_0(t) \simeq \frac{1}{6\pi^2 n} \int_0^{\infty} dk k^2 F_s(k,t) [C_L(k,t) + 2C_T(k,t)], \quad (1)$$

where $k^2 dk / (6\pi^2) = (1/3)d^3k / (2\pi)^3$, $F_s(k,t) = \langle \exp(ik \cdot [r(t) - r(0)]) \rangle$ is the self-intermediate scattering function of the tagged particle, and $C_L(k,t)$ and $C_T(k,t)$

are, respectively, the longitudinal and transverse current correlation functions:

$$j_L(\mathbf{k}, t) = \sum_{j=1}^{N_0} \frac{\mathbf{v}_j \cdot \mathbf{k}}{k} e^{i\mathbf{k} \cdot \mathbf{r}_j} = \mathbf{j}(\mathbf{k}, t) \cdot \frac{\mathbf{k}}{k}, \quad (2)$$

$$\mathbf{j}_T(\mathbf{k}, t) = \mathbf{j}(\mathbf{k}, t) - j_L(\mathbf{k}, t) \frac{\mathbf{k}}{k}, \quad (3)$$

$$C_L(k, t) = \frac{1}{N_0} \langle j_L(-\mathbf{k}, 0) j_L(\mathbf{k}, t) \rangle, \quad (4)$$

$$C_T(k, t) = \frac{1}{2N_0} \langle \mathbf{j}_T(-\mathbf{k}, 0) \cdot \mathbf{j}_T(\mathbf{k}, t) \rangle. \quad (5)$$

Using the hydrodynamic expressions $F_s(k, t) \sim \exp(-k^2 Dt)$ and $C_T(k, t) \sim v_T^2 \exp(-k^2 vt)$, valid for small k and large t (here $v_T^2 = k_B T/m$, so v_T is the characteristic thermal velocity of the particle), one gets the long-time tails from the transverse part of the expression Eq. (1). It has been shown that the predicted prefactor is very accurate as verified by numerical simulations in three dimensions [20].

The validity of Eq. (1) is restricted to the long- t domain. The so-called ‘‘velocity field approach’’ developed in Ref. [22] extends this formula to the short-time domain by inserting a ‘‘gate factor’’ $f(k)$ into the integral. However, the applicability of this formula, even in its extended form, is restricted to a density domain where the long-time tails are fully developed. When the density is increased, the viscosity also increases, and the prefactor of the long-time tail of the VAF decreases to small values, whereas a negative excursion of the VAF develops (decaying as $t^{-5/2}$). In that case, the (necessarily positive) long-time tail becomes an ultimate regime relevant for very large times only, and with a negligible magnitude. There is a matching density domain where the velocity field approach and the density fluctuation approach should be both alone insufficient to account for the properties of the VAF. This crossover domain is studied in detail in Ref. [23] using the so-called generalized kinetic theory [24]. This somewhat complicated theory succeeds in having in the same formula contributions arising from density fluctuations relaxations and coupling to the hydrodynamic field; such a result would be impossible to get at the level of the simple MCT approach because the different symmetries of the global fields involved prevent a general description of their combined effect.

To conclude, let us stress again that for a *dense* simple fluid, the above hMCT describes an effect which is, in principle, at work, but has tiny consequences on the VAF and the diffusional properties of the particles.

B. A single polymer in a θ solvent

We are primarily interested in polymer melts, but it is instructive to study first a single polymer in a θ solvent and the motion of its c.m. It is well known that the hydrodynamic interactions, which are typically long-ranged, yield a diffusion coefficient $\propto 1/\sqrt{N}$ [2,25]. It is also interesting to see the spreading out over time of these interactions by looking at the c.m. VAF $C_{c.m.}(t)$ of the polymer. Having in mind the preeminence of hydrodynamic coupling we are led to adapt the hMCT for simple liquids to the c.m. motion, *even if the monomeric density is high* (we stay, however, in the liquid range to keep a well-defined time scale separation between

the microscopic and mesoscopic regimes). Roughly speaking, the reason for that is that momentum fluctuations are lost very rapidly by diffusion for a single particle, but these fluctuations are ‘‘recycled’’ by other monomers for the polymer c.m.

The hydrodynamic-based MCT adapted to the polymer c.m. is quite simple: One projects the c.m. velocity V_x onto the bilinear variables $D_{\alpha, \mathbf{k}} = \rho_0(-\mathbf{k}) j_{\alpha}(\mathbf{k})$, where $\rho_0(\mathbf{k}) = \sum_{j=1}^N \exp(i\mathbf{k} \cdot \mathbf{r}_j)$ is the density fluctuation of the polymer chain for wave vector \mathbf{k} . In analogy to Eq. (1), one gets the following result for the c.m. VAF:

$$C_{c.m.}(t) \simeq \frac{1}{3nN} \int \frac{d^3k}{(2\pi)^3} F(k, t) [2C_T(k, t) + C_L(k, t)], \quad (6)$$

where n is the number density of solvent molecules, $F(k, t)$ is the dynamical form factor of the polymer chain,

$$F(k, t) \equiv \frac{1}{N} \langle \rho_0(-\mathbf{k}, 0) \rho_0(\mathbf{k}, t) \rangle,$$

and C_T and C_L are the current correlation functions for the solvent. The long-time regime is obtained by considering the integral for small k and large t . We can thus use the hydrodynamic limit of $C_T(k, t)$ which is given by

$$C_T(k, t) \simeq v_T^2 \exp(-k^2 v_s t), \quad (7)$$

where $v_T^2 \equiv k_B T/m$ and $v_s = \eta_s/\rho_s$ is the kinematic viscosity of the solvent [21,24] ($\rho_s = nm$ is the solvent mass density). As regards the dynamical form factor $F(k, t)$, one should apply the results of the Zimm theory [2], which predicts a scaling of the form $F(k, t) = F(k) \varphi_Z(Ak^3 t)$ (the scaling function φ_Z differs from that of the Rouse theory, termed φ in Ref. [10]). The precise form of the scaling function φ_Z does not matter because the decay of $C_{c.m.}(t)$ is governed by the time dependence of $C_T(k, t)$. The longitudinal component $C_L(k, t)$, on the other hand, gives negligible contributions and can be discarded.

On using the Gaussian static form factor for $F(k)$ [2],

$$F(k) = N f_D(Nb^2 k^2/6), \quad (8)$$

$$f_D(x) = \frac{2}{x^2} (e^{-x} - 1 + x), \quad (9)$$

we get two regimes for $C_{c.m.}(t)$ ($R_g = \sqrt{Nb^2/6}$ is the gyration radius of Gaussian chains [2]):

$$C_{c.m.}(t) \simeq \begin{cases} \frac{2}{\pi^{3/2}} \frac{v_T^2}{Nnb^2 \sqrt{v_s t}} & \text{if } v_s t \ll R_g^2, \\ \frac{1}{12\pi^{3/2}} \frac{v_T^2}{n(v_s t)^{3/2}} & \text{if } v_s t \gg R_g^2. \end{cases} \quad (10)$$

These results have also been obtained in Ref. [26].

The physical interpretation of this result is quite simple: Following Onsager’s regression hypothesis [27] a typical c.m. velocity fluctuation recedes like the mean relaxation upon a small uniform velocity initially given to each monomer of the chain [11]. (Note that this statement also rigorously and naturally comes from the FDT.) Within this picture, one interprets the first regime as a stage where the vorticity induced by the initial fluctuation spreads among the monomers and the solvent comprised inside R_g . More precisely, the hydrodynamic diffusion length $\ell_s(t) \sim \sqrt{v_s t}$ defines roughly the length scale over which the momentum is spread at time t . One can thus sketch the chain as a necklace of N/g dynamical blobs of radius $\ell_s(t)$ with $g \sim \ell_s(t)^2/b^2$ units in

each blob, so that the momentum fluctuation, initially located on the chain, is shared at time t among $N(t) = (N/g) n \ell_s(t)^3$ solvent particles. As a result, $C_{c.m.}(t) \sim C_{c.m.}(0)N/N(t) \sim 1/Nn\ell_s(t)$. The first regime stops when the dynamical blob is so large that it encompasses the whole chain: $\ell_s(t) \sim R_g$. The second regime corresponds to the usual long-time tail: One has $C_{c.m.}(t) \sim C_{c.m.}(0)N/(n\ell_s^3) = 1/n(v_s t)^{3/2}$ because the initial fluctuation is now shared by $n\ell_s^3$ particles [21].

Upon integration of $C_{c.m.}(t)$ over time one recovers a diffusion coefficient $\propto 1/\sqrt{N}$ in agreement with the Zimm prediction. Let us mention also that if the dynamics is not momentum-conserving, as for instance with a Langevin dynamics, all previous conclusions no longer hold. At the mode-coupling level, this is embodied by a factor $\exp(-\gamma t)$ (where γ is the Langevin friction constant) which decorates the transverse current correlation function; physically the momentum diffusion is screened beyond a length scale $\sqrt{v_s/\gamma}$, and the actual c.m. motion is Rouse-like at $t \gg 1/\gamma$. This may seem obvious, but interestingly, as we see below, it is *no longer true* for polymeric melts (see Sec. III).

C. Polymer c.m. diffusion in a melt

For a tagged chain diffusing in a melt the hydrodynamic effects highlighted in the preceding section are profoundly modified by the viscoelastic properties of the melt.

1. c.m. VAF relaxation

The starting point is Eq. (6), but by contrast with the polymer in a solvent, the transverse current correlation function $C_T(k, t)$ is that of a polymer melt. This is readily seen by inspecting the relationship between $C_T(k, t)$ and $E(t)$, the hydrodynamic limit (i.e., $k \rightarrow 0$) of the shear modulus [24]. For small values of k , one has (as in Ref. [10], the carets represent the Laplace transform of the corresponding functions)

$$\frac{\partial C_T(k, t)}{\partial t} = -\frac{k^2}{nm} \int_0^t dt' E(t') C_T(k, t - t'), \quad (t > 0) \quad (11)$$

$$\widehat{C}_T(k, z) = \frac{v_T^2}{z + \frac{k^2}{nm} \widehat{E}(z)}, \quad (12)$$

where n is now the monomer number density of the melt, $v_T^2 = k_B T/m$, and m is the monomer mass; note that $C_T(k, 0) = v_T^2$, as follows directly from the Gibbs statistics. For a polymeric melt described by the Rouse model, the shear relaxation modulus $E(t)$ is given by the following relation:

$$E(t) \simeq \frac{nmv_T^2}{\sqrt{2\pi^2 W t}}, \quad t_1 \ll t \ll t_N. \quad (13)$$

This formula is valid for times longer than the monomer time $t_1 = 2/(\pi^3 W)$ and smaller than the Rouse time $t_N = N^2 t_1$. (We define the time constant W^{-1} by postulating that in this regime the monomer MSD is $\delta h_0(t) = b^2 \sqrt{W t}$, where b is the statistical segment length [10].)

Using Eqs. (11)–(13) we find the following scaling form for the transverse current correlation function valid for $t_1 \ll$

$t \ll t_N$ [28]:

$$C_T(k, t) = v_T^2 \zeta(a^{2/3} k^{4/3} t), \quad (14)$$

$$\widehat{\zeta}(z) = \frac{\sqrt{z}}{z^{3/2} + 1}, \quad (15)$$

where $a = v_T^2/\sqrt{2\pi W}$. Disregarding once more the longitudinal current (its contribution is always subdominant and vanishes in the incompressible limit), we get

$$C_{c.m.}(t) \simeq \frac{2v_T^2}{3nN} \int \frac{d^3 k}{(2\pi)^3} F(k) \varphi(Ak^4 t) \zeta(a^{2/3} k^{4/3} t). \quad (16)$$

Note that here we used the following approximation for the dynamical form factor valid for $t_1 \ll t \ll t_N$ (see Ref. [10]):

$$F(k, t) = F(k) \varphi(Ak^4 t), \quad A = \frac{\pi b^4 W}{144} \quad (17)$$

where

$$\varphi(y) = \sqrt{y} \int_0^\infty du \exp[-\sqrt{y} H(u)], \quad (18)$$

$$H(u) = u + \frac{2}{\pi} \int_0^\infty \frac{dx}{x^2} (1 - e^{-x^2}) \cos(xu). \quad (19)$$

By construction, Eq. (16) addresses the long-time regime ($t \gg t_1$), characterized by the relaxation of large structures. As a result, only the small- k region (defined by the ζ factor in the integrand) is relevant in the preceding equation: $k \sim a^{-1/2} t^{-3/4}$. Hence, $Ak^4 t \sim b^4 W^2/(v_T^4 t^2) \ll 1$ (since $t \gg t_1$ and $v_T t_1 \gg b$), so that the φ factor in Eq. (16) can be replaced by $\varphi(0) = 1$.

A qualitative analysis of Eq. (16) is useful, as it shows the important features of the MCT prediction. For large enough $y = a^{2/3} k^{4/3} t \gg 1$, we have $\zeta(y) \sim -y^{-3/2}/(2\sqrt{\pi})$ [see Eq. (15)]. As regards the form factor, the scale-free intrachain regime of low k is given by $F(k) = 12/(kb)^2$. Then, we get that $C_{c.m.}(t) \propto N^{-1} t^{-3/2} \int_{k \geq 1/R_g} dk/k^2 \propto N^{-1/2} t^{-3/2}$, where the lower bound of the integral for k is defined by the chain size R_g . Thus, an intermediate prediffusive regime is predicted which dominates largely (due to the factor $N^{-1/2}$) both the Rouse behavior and the dMCT result [10]. This analysis emphasizes the dominant role played by the typical lengths $\propto \sqrt{N}$ comparable to the chain size.

To go into more detail, we find using Eq. (16)

$$C_{c.m.}(t) \simeq \frac{v_T^2}{nb^3 N^{3/2}} \frac{\sqrt{24}}{\pi} f_0(t/\tau), \quad (20)$$

$$\tau = \left(\frac{\pi}{18}\right)^{1/3} \left(\frac{Nb^2 \sqrt{W}}{v_T^2}\right)^{2/3}, \quad (21)$$

$$f_0(X) = \frac{2}{\pi} \int_0^\infty dy \zeta(Xy^{4/3}) \frac{e^{-y^2} - 1 + y^2}{y^2}, \quad (22)$$

where $t/\tau = a^{2/3} t R_g^{-4/3} \sim t N^{-2/3}$ emerges as the scaling variable. The above equation is valid for $t_1 \ll t \ll t_N$. Two limiting behaviors are obtained in the limits $t/\tau \ll 1$ and

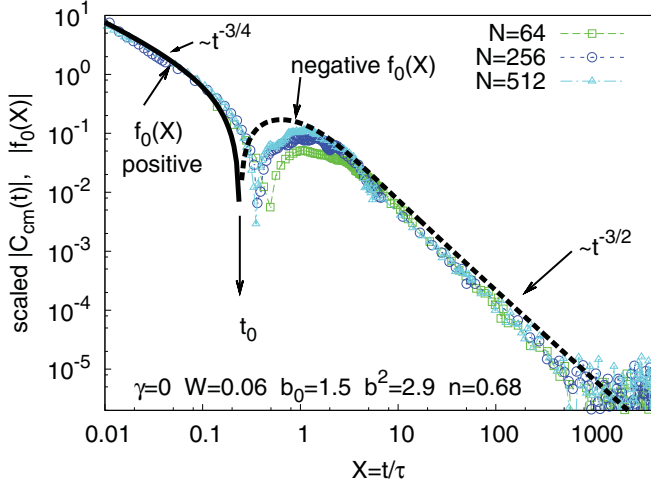


FIG. 1. (Color online) Comparison between the theoretical scaling function $|f_0(X)|$ (solid line, positive part; dashed line, negative part), and the simulation data for $N = 64, 256,$ and 512 (squares, circles, and triangles, respectively), for model (A) (described in Ref. [10]) under momentum-conserving dynamics; the simulation curves represent $nb^3 N^{3/2} \pi |C_{c.m.}(t)| / (\sqrt{24} v_T^2)$ as a function of t/τ . The vertical arrow indicates the predicted sign inversion at $X \simeq 0.24$.

$t/\tau \gg 1$:

$$C_{c.m.}(t) \underset{t/\tau \ll 1}{\simeq} + \frac{2^{5/4}}{\Gamma(\frac{1}{4})\pi^{3/4}} \frac{v_T b W}{N n b^3} (Wt)^{-3/4}, \quad (23)$$

$$C_{c.m.}(t) \underset{t/\tau \gg 1}{\simeq} - \frac{4}{(3\pi)^{3/2}} \frac{W^2 b^2}{n b^3} \frac{(Wt)^{-3/2}}{\sqrt{N}}. \quad (24)$$

This is the main result of this section.

2. Comparison to numerical simulations

To get the whole temporal evolution, one inverts the relation (15) and gets

$$\zeta(y) = \frac{4}{3} e^{-y/2} \cos\left(\frac{\sqrt{3}}{2} y\right) - \frac{1}{\pi} \int_0^\infty du e^{-uy} \frac{\sqrt{u}}{u^3 + 1}, \quad (25)$$

whence we numerically compute $f_0(X)$, plotted in Fig. 1. Note that $C_{c.m.} > 0$ for $X < X_0 \approx 0.24$ (i.e., $t < t_0 \approx 0.24\tau$) and $C_{c.m.} < 0$ for $t > t_0$. Thus, when comparing with numerical or experimental data, one would take advantage to represent the data according to the somewhat unexpected scaling $N^{3/2} C_{c.m.}(t)$ vs $t/N^{2/3}$ suggested by the result (20).

The theoretical curve in Fig. 1 is compared with computer simulation data obtained with momentum conserving dynamics. One can observe a perfect agreement of the scaling of the different chain lengths in the long time regions which is responsible for the subdiffusive motion in the c.m. as shown later in Sec. II C 4. The agreement with the theoretical curve is very good apart from some mismatch at the sign inversion time t_0 , but this mismatch tends to diminish as the chain length N is increased. The bead-spring chains have increased bond length $b_0 = 1.5\sigma_{LJ}$ to be able to test the theory for arbitrarily long unentangled chains. Details about the model (A) used for these simulations can be found in the first part of this series [10]. Let us stress, however, that here we used a large

box ($L \approx 83\sigma_{LJ}$ for $N = 256$ and $L \approx 105\sigma_{LJ}$ for $N = 512$) with 1536 chains to avoid significant box-size effects which occur for smaller systems. The simulation is run with a weak pair-friction introduced in the context of dissipative particle dynamics together with the full repulsive LJ potential as discussed in Ref. [29]. This serves essentially for the long-time stability of the numerical integration.

3. Physical interpretation

Let us comment on the physical meaning of the obtained scaling function. It reflects the effect of hydrodynamic interactions including both the inertial and the viscoelastic responses of the melt. As in Sec. II B and in Ref. [11], Onsager's regression hypothesis (or the FDT) is helpful in drawing a physical picture of the MCT results (we recall that the FDT also makes it possible to derive the same quantitative results we derived here via the hMCT; see [11] for details on the FDT derivation): The c.m. VAF is proportional to the velocity field evolution (averaged over initial conformations of the chain) of the c.m. of a tagged chain after an instantaneous pushing force $\mathbf{p}_0 \delta(t) \delta(\mathbf{r} - \mathbf{r}_i)$ applied to every monomer \mathbf{r}_i of the tagged chain:

$$\langle \mathbf{V}_{c.m.}(t) \rangle = \frac{N}{k_B T} C_{c.m.}(t) \mathbf{p}_0. \quad (26)$$

The dynamics of the velocity field is given by the generalized incompressible Navier-Stokes equation (linearized because we are by definition close to equilibrium),

$$\rho \partial_t \mathbf{v} = -\nabla P + \int_0^t dt' E(t-t') \Delta \mathbf{v}(t') + \mathbf{p}_0 \delta(t) \sum_{j=1}^N \delta[\mathbf{r} - \mathbf{r}_j(0)], \quad (27)$$

$$\nabla \cdot \mathbf{v} = 0, \quad (28)$$

where $\rho = nm$ is the mass density of the melt. The viscosity term in this generalized Navier-Stokes equation is an integro-differential term accounting for the viscoelastic properties of the fluid [30]. Doing so, we consider the tagged chain as being an ordinary element of the melt and treat the external force as being applied to the whole viscoelastic medium. This extrapolation is commonplace in liquid-state physics, where it is well known that hydrodynamics is still valid at fairly short length scales. It is worth stressing that such a procedure would not apply to the relaxation of a single monomer of a tagged chain (to get by the same method the monomeric VAF relaxation) because the intrachain forces in that case are obviously not negligible (the negligible effect of hydrodynamic flow on the monomer motion is examined in Sec. V). By contrast, for the c.m. motion, the intrachain forces sum up to zero by virtue of the Newton's third law, and one can expect that the connectivity plays a negligible role. In addition, it is important that the diffusion of the chain elements with respect to the main hydrodynamic flow can be neglected because the momentum diffusion is much faster than the monomer motion, a fact embodied by the irrelevance of the time dependence of $F(k,t)$ in Eq. (16). As a result, there is no important coupling between the hydrodynamic flow and the structural relaxation of the *tagged* chain, and the

MCT assumption of the factorization of four-point dynamic correlators is actually not required.

The solution of Eq. (27) is by linearity the sum of the flows induced by the individual kicks. Qualitatively, these individual flows correspond to the spreading of the initial momentum carried by an initial kick. For a Newtonian fluid, this spreading is simple and can be summarized as in Sec. II B: The momentum is homogenized at time t over a diffusion spot of typical size $\ell_s(t) \sim \sqrt{v_s t}$.

For a polymeric melt this spreading is much more complex: First, the momentum diffusion length $\ell(t)$ is influenced by the growth in time of the effective viscosity $\eta(t) = \int_0^t E(t') dt' \sim k_B T n \sqrt{t/W}$. In that case, a natural guess for the diffusion length is $\ell(t) = (2\pi)^{-1/4} \sqrt{\eta(t)t/\rho} = v_T [2\pi W]^{-1/4} t^{3/4}$ (the numerical prefactor is here for sake of coherence with the following development). We see that the momentum “superdiffuses” because of the gradual increase of the viscosity. Second, the momentum distribution inside the diffusion spot [of size $\ell(t)$] is strongly heterogeneous, in marked contrast with the Newtonian fluid. We can see this as follows. Suppose that a kick $\mathbf{p}_0 \delta(t) \delta(\mathbf{r})$ is given at the origin $\mathbf{r} = 0$ to a polymer melt. A physically relevant observable is the momentum density at distance R at time t , averaged over all directions. From Eq. (27) we find that this observable can be written as $Q_{\text{melt}}(R, t) \ell(t)^{-3} \mathbf{p}_0$, with [31]

$$Q_{\text{melt}}(R, t) = \frac{1}{3\pi} \left(\frac{\ell(t)}{R} \right)^{13/3} Q_0([\ell(t)/R]^{4/3}), \quad (29)$$

$$\widehat{Q}_0(z) = (1 + z^{3/4}) e^{-z^{3/4}}. \quad (30)$$

From the scaling variable we recover exactly the growing momentum diffusion length, $\ell(t) = (2\pi)^{-1/4} \sqrt{\eta(t)t/\rho}$, introduced above. For a Newtonian fluid the same orientation-averaged momentum density is given by $Q_{\text{fluid}}(R, t) \ell_s(t)^{-3} \mathbf{p}_0$ with

$$Q_{\text{fluid}}(R, t) = \frac{1}{2\pi} \left(\frac{\ell_s(t)}{R} \right)^5 Q_1([\ell_s(t)/R]^2). \quad (31)$$

$$\widehat{Q}_1(z) = (1 + \sqrt{z}) e^{-\sqrt{z}}. \quad (32)$$

In Fig. 2 the scaled averaged momentum densities $Q_{\text{melt}}(R, t)$ and $Q_{\text{fluid}}(R, t)$ are shown as a function of their respective scaling variables $R/\ell(t)$ and $R/\ell_s(t)$. One can clearly see that the momentum distribution inside the diffusion spot is positive and rather homogeneous for a Newtonian fluid, in accordance with the traditional picture of a normal diffusion and rather flat repartition of momentum inside the spot of size $\ell_s(t)$. On the contrary, the momentum repartition within $\ell(t)$ for the melt is strongly inhomogeneous: It displays a central core of negative momentum surrounded by an external shell of positive momentum. The central negative shell comes from the fact that the advancing front of momentum diffusion shears the melt and leaves a storage of some elastic free energy due to nonoptimal (sheared) conformations of the local chains. This stored energy is afterward released by the recoiling of the stretched chains, which induces a negative remnant in the momentum distribution in the “aged” regions within the diffusion spot. Note that the recoiling of the central core leads necessarily to an enhancement of the positive momentum stored in the outer shell (with respect to the total momentum transferred to the melt). This phenomenon is analogous to the

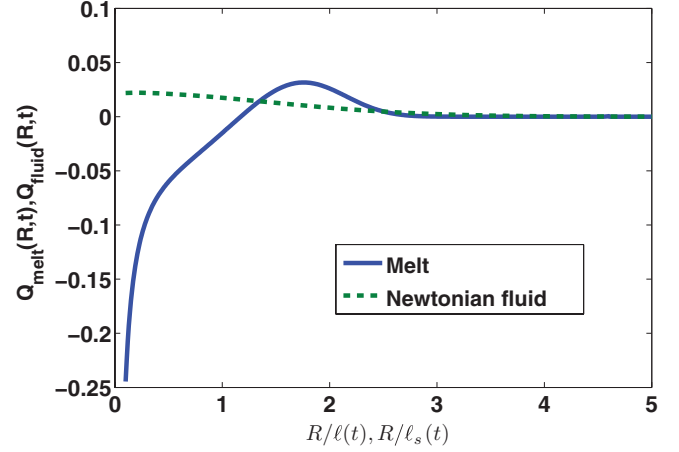


FIG. 2. (Color online) Orientation-averaged scaled momentum distribution inside a fluid [viscoelastic melt, $Q_{\text{melt}}(R, t)$, solid line; Newtonian fluid, $Q_{\text{fluid}}(R, t)$, dashed line] after an initial localized kick (see text for details). Note the different definition of the abscissa in both cases: $R/\ell(t)$ for the melt and $R/\ell_s(t)$ for the Newtonian fluid. Note also that $Q_{\text{melt}}(R, t) \propto \ell(t)/R$ near $R/\ell(t) = 0$.

so-called *elastic recoil* in the classical rheological properties of polymeric fluids [32], where the cessation of a shear flow in a complex fluid is typically followed by a flow reversal.

If we go back to the physical interpretation of Eqs. (23) and (24), the above analysis and the FDT lead to the following picture: In the time range $t_1 \ll t \ll 0.24\tau$, the tagged chain can be seen as a necklace of $N/g(t)$ dynamic blobs of size $\ell(t)$ with nearly uniform velocity [$g(t)$ is related to $\ell(t)$ by $g(t) \sim \ell(t)^2/b^2$]. The fraction of initial momentum still borne by the chain at time t is thus $C_{c.m.}(t)/C_{c.m.}(0) \sim N/(n \frac{N}{g(t)} \ell(t)^3) \propto N^0 n^{-1} t^{-3/4}$, in agreement with Eq. (23). Of course, we emphasized above that the momentum distribution within the dynamic blob is not “nearly uniform.” However, in the first time regime this inner structuring of the diffusion blob may be neglected (because the distribution of the blobs along the chain backbone leads to a spatial averaging over the distance R). This initial regime (23) ceases as soon as $\ell(t)$ reaches the chain size $R_g \sim b\sqrt{N}$: This corresponds to the typical time $\tau \sim N^{2/3}$. For $t \gg \tau$, the whole chain is henceforth included in the recoiling remnants of the N initial kicks. However, now the velocity field due to each kick is not nearly uniform at length scales less than or comparable to the chain size. For large t we have $Q_{\text{melt}}(R, t) \sim -\ell(t)/R$, whence we get from Eq. (26) a final relaxation $C_{c.m.}(t) \sim -N^{-1} \frac{N}{n(N^{3/2}b^3)} \frac{b^2 N}{[\ell(t)^2]} \sim -\frac{1}{n\sqrt{N}b\ell(t)^2}$, which is Eq. (24) up to a numerical factor. Note that the nonuniform momentum distribution $Q_{\text{melt}}(R, t) \sim -\ell(t)/R$ in the recoil zone is directly related to the exponent $t^{-3/2}$ in Eq. (24). This last point stresses the relative complexity of the viscoelastic relaxation even in the second stage where the screening length $\ell(t)$ is, however, larger than the chain size.

Here it is worth stressing that one must not confuse this viscoelastic recovery regime (*negative* tail with an exponent $-3/2$) with the ordinary long-time tail in a simple fluid as exemplified by the second regime of Eq. (10) (*positive* tail with an exponent $-3/2$), the common exponent being rather accidental. In the simple fluid, the factor 3 comes from the

space dimension d ; the exponent, $-3/2$, in the polymer melt comes entirely from the stress relaxation law $E(t) \propto 1/\sqrt{t}$ which is unrelated to d .

An alternative and complementary interpretation of the results of Eqs. (23) and (24), based on an analysis of the mobility of the chain and on a time-dependent generalization of the Oseen tensor, is given in Sec. IV.

4. c.m. mean-square displacement

To conclude this section we determine the c.m. MSD of the tagged chain

$$h_{c.m.}(t) = \frac{1}{6} \langle [\mathbf{R}_{c.m.}(0) - \mathbf{R}_{c.m.}(t)]^2 \rangle \quad (33)$$

by using the general relation $C_{c.m.}(t) = \frac{\partial^2}{\partial t^2} h_{c.m.}(t)$, which follows directly from the definition of the functions $h_{c.m.}(t)$ and $C_{c.m.}(t)$. Using these relations and the results obtained in this section we get in the regime $\tau \ll t \ll t_N$:

$$h_{c.m.}(t) \simeq b^2 \left[\frac{\pi}{12} \frac{Wt}{N} + \frac{16}{(3\pi)^{3/2}} \frac{1}{nb^3} \left(\frac{Wt}{N} \right)^{1/2} \right]. \quad (34)$$

Here the first Fickian term represents the Rouse result, while the second term is due to the VHIs. It is clear that the cooperative flow (VHI) contribution dominates the c.m. MSD for short times, that is, for

$$t \lesssim \frac{4.5}{(nb^3)^2} \frac{N}{W} \equiv t^{**}. \quad (35)$$

Therefore, roughly speaking $h_{c.m.}(t) \propto \sqrt{t}$ for $t \lesssim t^{**}$ and $h_{c.m.} \propto t$ for $t \gtrsim t^{**}$. Note that the crossover time t^{**} scales as the geometric average of monomer time t_1 and Rouse time t_N : $t^{**} \sim \sqrt{t_1 t_N}$. The apparent dynamical exponent $z = \frac{\partial \ln h_{c.m.}(t)}{\partial \ln t}$, therefore, changes from 0.5 to 1, the average value (on the long-time scale) being $\bar{z} \simeq 0.75$, which is rather close to what is actually observed in numerical or experimental works [3–8]: $z \approx 0.75-0.85$.

The asymptotic exponent $z = 0.5$ will be rarely visible on the MSD, not only because of the superposition with the Fickian term at long times, but also because of the crossover from the superdiffusive regime at early times. Figure 3 summarizes the results by showing the c.m. MSD for the whole time domain, superposing different chain lengths of model (A) (data obtained with momentum conserving dynamics). In the initial ballistic regime, $Nh_{c.m.}(t) \sim t^2$. Then, the first relaxation regime of the c.m. VAF [Eq. (23)] leads to a superdiffusive regime $Nh_{c.m.}(t) \sim t^{5/4}$ until the viscoelastic spreading of momentum goes beyond the chain size at $t_0 \approx 0.24\tau \sim N^{2/3}$. Then, the second relaxation regime due to viscoelastic recovery Eq. (24) leads to the subdiffusive motion described by Eq. (34). Note that the acceleration during the first superdiffusive regime is canceled by the second subdiffusive regime, so that at the end, the prediction of the Rouse model, $h_{c.m.}(t) \sim t/N$, is recovered.

Figure 4 shows the same representation for a bead-spring model with conserved topology (again the data were obtained with momentum conserving dynamics and with 1536 chains per system). At early times, the same behavior is found with a first superdiffusive regime followed by the subdiffusive regime. The situation becomes different around the entanglement time $\tau_e \approx 3000$. The short chain, $N = 64$, enters the

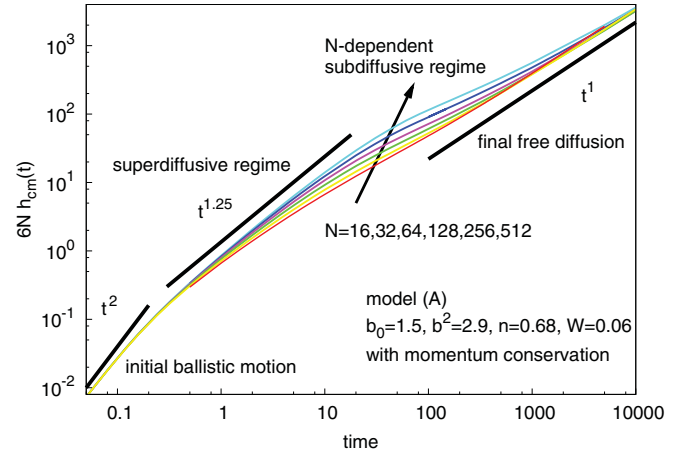


FIG. 3. (Color online) MSD of the c.m., multiplied by the chain length N , for model (A) of Ref. [10] (chains can cross each other because of the increased bond length $b_0 = 1.5\sigma_{LJ}$; these are the same data sets as used for the inset in Fig. 1 of Ref. [11]). In this representation, the curves superpose for early times and in the final diffusive regime. In the intermediate time, the curves split up: The first superdiffusive regime caused by the spreading of momentum lasts until $\tau \propto N^{2/3}$. After the c.m. VAF has changed sign, the subdiffusive signature is strongest, crossing over continuously to the free diffusion beyond the Rouse time.

free diffusion here, whereas the longest chain, $N = 1024$, continues with $h_{c.m.}(t) \sim t^{0.5}$ as expected from the tube theory for entangled motion [8]. The c.m. VAF shown in the inset has exactly the same signature as for the unentangled model. The results derived in this section are thus fully applicable

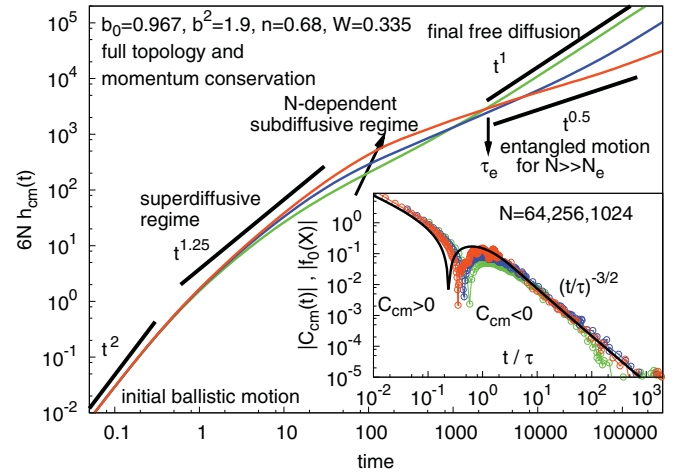


FIG. 4. (Color online) MSD of the c.m. for the standard bead-spring model with conserved topology (bond length $b_0 = 0.967\sigma_{LJ}$). The data are multiplied by chain length ($N = 64$, green; $N = 256$, blue; $N = 1024$, orange). The same representation as in Fig. 3 shows that the VHI effects are present in the equivalent time windows up to the entanglement time. The shortest chain, $N = 64$, crosses over directly to free diffusion, whereas the longest chain, $N = 1024$, enters the entangled regime for which tube theory would predict a power law of $t^{0.5}$. The inset shows the c.m. VAF in the same representation as Fig. 1, indicating excellent agreement between the theoretical scaling function $|f_0(t/\tau)|$ (black line) and the simulations.

to entangled melts in the early time regime, at least as long as $\tau < \tau_e$, which appears to be the case for a wide range of loosely entangled melts.

III. C.M. DIFFUSION IN A MELT UNDER NON-MOMENTUM-CONSERVING DYNAMICS

The preceding considerations highlighted the prominent role played by the viscoelastic properties of the melt for the c.m. relaxation, which have been captured solely by the hMCT. A slightly paradoxical consequence of this finding is that the hMCT is relevant also for *non-momentum-conserving dynamics*. Let us consider first melt systems whose dynamics is defined by a coupling with a Langevin thermostat providing the Langevin friction force $\mathbf{f}_L = -\gamma m \mathbf{v}$ on each monomer moving with velocity \mathbf{v} (and the corresponding white noise force). The case of a Monte Carlo dynamics is discussed later.

A. hMCT for Langevin dynamics

1. Analytical expressions

The hMCT in this case is still embodied by Eq. (6), although the physical relevance of this equation may be questioned, since the transverse current is no longer a conserved quantity. For instance, we already mentioned that for a single polymer in a low-molecular solvent, the transverse current correlation function recedes exponentially with a rate γ corresponding to the Langevin friction. However, this is no longer true for $k \neq 0$ in polymer melts. In fact, to define $C_T(k, t)$ in this case we employ Eq. (11) modified with the friction term (this can be justified by considering a Mori-Zwanzig theory applied to the stochastic Kramers propagator):

$$\frac{\partial C_T(k, t)}{\partial t} \Big|_{t>0} = -\frac{k^2}{\rho} \int_0^t dt' E(t') C_T(t-t') - \gamma C_T(k, t). \quad (36)$$

Applying a Laplace transform, we get

$$\widehat{C}_T(k, z) = \frac{v_T^2}{z + \gamma + \frac{k^2}{\rho} \widehat{E}(z)}. \quad (37)$$

Note that here we neglect the k dependence of the relaxation modulus E (see Appendix A).

Let us consider the most important regime, when the time is longer than the Langevin relaxation time γ^{-1} (the results for $\gamma t \sim 1$ are outlined in Appendix B). Then, the transverse current correlation function has the following scaling form:

$$C_T(k, t) = -\frac{A v_T^2}{\gamma \bar{\gamma}^2} k^4 C_1(A k^4 \bar{\gamma}^{-2} t), \quad (38)$$

$$\bar{\gamma} = \frac{m\gamma}{\zeta_1}, \quad (39)$$

$$\widehat{C}_1(z) = -\frac{\sqrt{2z}}{\sqrt{2z} + 1}, \quad (40)$$

$$C_1(y) = \frac{1}{\sqrt{2\pi y}} - \frac{1}{2} \operatorname{erfcx}(\sqrt{y/2}), \quad (41)$$

where $\zeta_1 = \frac{12}{\pi} k_B T b^{-2} W^{-1}$ is the effective monomer friction constant, $\operatorname{erfcx}(y) = e^{y^2} \frac{2}{\sqrt{\pi}} \int_y^\infty du e^{-u^2}$, and A is defined in Eq. (17). The limiting behavior of $C_1(y)$ is $(2\pi y)^{-1/2}$ for $y \ll 1$ and $(2\pi y^3)^{-1/2}$ for $y \gg 1$. The parameter $\bar{\gamma}$ is just

the ratio of the Langevin friction constant $m\gamma$ to the overall effective monomer friction constant ζ_1 ; therefore, $\bar{\gamma} < 1$ by definition. Note also that $\bar{\gamma} = \frac{\pi}{12} \frac{b^2 W \gamma}{v_T^2}$. Hence, alternatively, $\bar{\gamma}^{-1}$ can be viewed as the ratio of the Langevin diffusion coefficient v_T^2/γ to the “dressed” monomeric diffusion coefficient $D_1 = N D_N = \pi b^2 W/12$ emerging in the long-time diffusion regime.

As a result, the scaling behavior of $C_T(k, t)$ is substantially altered by the Langevin friction, but not wiped out. The scaling form Eq. (38) shows moreover an important feature: If $\bar{\gamma} \ll 1$, only small values of $A k^4 t$ yield non-negligible values of $C_T(k, t)$. This implies that the dynamical form factor $F(k, t) = F(k) \varphi(A k^4 t)$ can be replaced by the static value $F(k)$ in Eq. (6). A second major consequence of the assumption $\bar{\gamma} \ll 1$ is that in that case, the ansatz $E(k, t) \simeq E(t)$ is automatically valid (see Appendix A; note that the case $\bar{\gamma} \ll 1$ encompasses the conserving dynamics of Sec. II C, equivalent to the limiting case $\bar{\gamma} = 0$). We restrict the discussion in the next section to such systems with $\bar{\gamma} \ll 1$ (other cases are considered in Sec. III B).

2. c.m. VAF for small dressed Langevin friction $\bar{\gamma}$

The simplifications afforded by the hypothesis $\bar{\gamma} \ll 1$ induce in Eq. (6) a rather simple scaling behavior for $C_{c.m.}(t)$ provided $t \gg \gamma^{-1}$:

$$C_{c.m.}(t) = -\frac{b^2 W^2 \bar{\gamma}^{-3}}{4\sqrt{6} n b^3 N^{7/2}} f_1[\pi \bar{\gamma}^{-2} W t / (4N^2)], \quad (42)$$

$$f_1(y) = \int_0^\infty dx x^6 f_D(x^2) C_1(y x^4). \quad (43)$$

For $\bar{\gamma} \ll 1$, the relaxation of $C_{c.m.}(t)$ displays two regimes beyond the time $\sim \gamma^{-1}$: For small times, we get

$$C_{c.m.}(t) \simeq -\frac{(Wt)^{-5/4} b^2 W^2}{N n b^3} \xi(\bar{\gamma}), \quad (44)$$

$$\xi(\bar{\gamma}) \underset{\bar{\gamma} \ll 1}{\simeq} \frac{\Gamma(1/4)}{\underbrace{2^{9/4} \sqrt{3\pi}^{5/4}}_{\simeq 0.1052}} \bar{\gamma}^{-1/2}. \quad (45)$$

Let us remark here that this power-law regime is *identical* to that predicted by the dMCT, apart from the prefactor, a pure constant $\simeq 0.037$ for the dMCT (cf. Eq. (27) of Ref. [10]), a larger constant $\xi(\bar{\gamma})$ depending on the Langevin friction in the present case. However, this formal similarity does not mean that the physical ingredients implemented by the two versions of the MCT are the same. In the hMCT approach, the $-N^{-1} t^{-5/4}$ scaling regime lasts as long as the relevant length scale k^{-1} is smaller than the chain size.

For large times, $Wt \gg (N\bar{\gamma})^2$, the reduced transverse current correlation function is given by $C_1(A k^4 \bar{\gamma}^{-2} t) \propto \bar{\gamma}^3 k^{-6} t^{-3/2}$ for all k spanned by the form factor, and we rather have

$$C_{c.m.}(t) \underset{N^2 \gg Wt \gg (N\bar{\gamma})^2}{\simeq} -\frac{4}{(3\pi)^{3/2}} \frac{W^2 b^2 (Wt)^{-3/2}}{n b^3 \sqrt{N}}, \quad (46)$$

that is, the same formula as Eq. (24). Let us stress here that this regime can be well developed before the Rouse time only

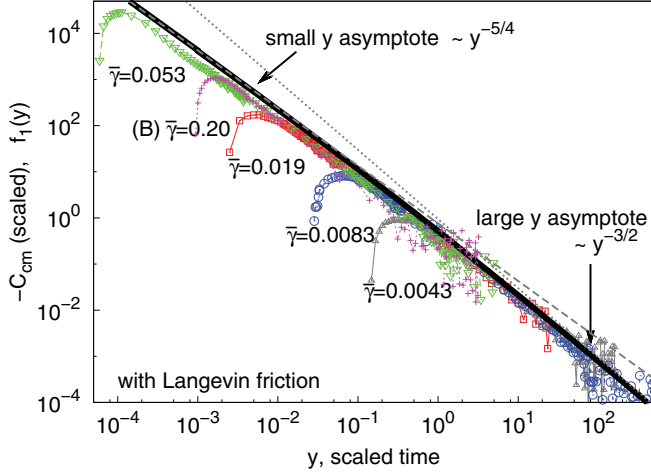


FIG. 5. (Color online) Plot of the scaling function $f_1(y)$ [Eq. (43), thick solid line] together with Langevin dynamics simulation data for the negative c.m. VAF of different systems to highlight the universality of the theoretical prediction. The asymptotic behavior of $f_1(y)$ is also indicated. For small y it is given by $2^{-1/4}\Gamma(5/4)y^{-5/4}$ (dashed line); for large y it is given by $3^{-1}\sqrt{8}y^{-3/2}$ (dotted line). The simulation data are scaled according to Eq. (42), the abscissa is $\pi\bar{\gamma}^{-2}Wt/4N^2$, and the ordinate is $-4\sqrt{6}nb^3N^{7/2}C_{c.m.}(t)/[b^2W^2\bar{\gamma}^{-3}]$. All simulation data refer to $N = 256$. The open symbols correspond to model (A) with increased bond length and the plus signs correspond to model (B) with softened excluded volume of Ref. [10]. For model (B), one data set is shown with the bare friction constant $\gamma = 0.5$; the other data sets correspond to model (A) with different friction strength (from left to right, $\gamma = 2.0, 0.5, 0.2, 0.1$); the figure indicates the corresponding dressed friction coefficient $\bar{\gamma}$.

if $\bar{\gamma} \ll 1$ (which is the case considered in this section). A well-defined crossover time (for $\bar{\gamma} \ll 1$) between the regimes (44) and (46) is $t^* \sim 3W^{-1}(N\bar{\gamma})^2$. This crossover is visible in Fig. 5 showing the function $f_1(y)$, together with the numerical simulations described in Ref. [10]. One clearly sees that the matching between theory and simulation is always very good, although there is a systematic overestimation by a factor $\simeq 0.7$ in the small- y region. Let us stress, however, that this slight discrepancy is by no means comparable with that found in Ref. [10], where a definitely subdominant mechanism was considered (see also Sec. III B).

3. The Langevin screening length

To understand the physical content of Eqs. (44) and (46), we follow the same lines as in Sec. II C. For a simple fluid, the Langevin friction, which makes the initial momentum fluctuation disappear within a characteristic time γ^{-1} , prevents also the spreading of the initial disturbance over large distances: The maximum length for the diffusion of momentum is given by the screening length $\sqrt{\eta/(\rho\gamma)}$ [33] (note, however, that in any case, the incompressibility of the fluid creates instantaneously a flow not strictly local after the initial, localized, kick).

This behavior is significantly altered in the case of a viscoelastic melt. Qualitatively, this is due to the fact that the instantaneous viscosity $\eta(t) = \int_0^t dt' E(t')$ evolves in time.

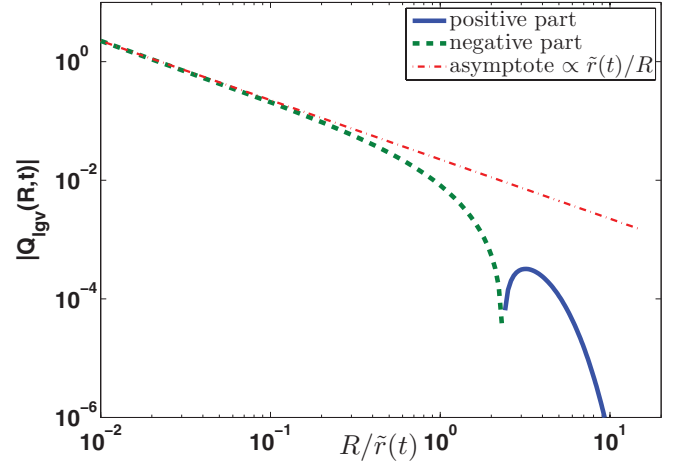


FIG. 6. (Color online) Scaled orientation-averaged momentum distribution inside a viscoelastic melt under Langevin dynamics (with $\bar{\gamma} \ll 1$) after an initial localized kick (see text for details).

As a result, the screening length $\tilde{r}(t)$ now grows with time,

$$\tilde{r}(t) = (2\pi)^{-1/4} \sqrt{\eta(t)/\rho\gamma} = b \left(\frac{Wt}{2\pi} \right)^{1/4} \bar{\gamma}^{-1/2}. \quad (47)$$

(As in Sec. II C, the numerical factor is here for the sake of consistency with the subsequent analysis.) Thus, one expects the fluid to be out of rest within a domain which increases with t . This is somewhat counterintuitive because the total momentum is destroyed by the Langevin friction within a typical time γ^{-1} : The spreading corresponds to a sort of sluggish anomalous propagation of the initial shear, not driven by the diffusion of momentum, but by a slow release of elastic conformational energy. To picture this idea in more detail we compute the same quantity as in Sec. II C, namely the momentum density at distance R and time t after an initial kick $\delta(t)\delta(\mathbf{r})\mathbf{p}_0$ (averaged over all directions). It can be written as $Q_{\text{lgv}}(R,t)(\gamma t)^{-1}\tilde{r}(t)^{-3}\mathbf{p}_0$ with

$$Q_{\text{lgv}}(R,t) = \frac{1}{4\pi} \left(\frac{\tilde{r}(t)}{R} \right)^7 Q_2([\tilde{r}(t)/R]^4), \quad (48)$$

$$\widehat{Q}_2(z) = \sqrt{z} \exp(-z^{1/4}). \quad (49)$$

We remark first that the length $\tilde{r}(t)$ defines properly a screening length associated with the spreading of an initial localized percussion. The sketch of $Q_{\text{lgv}}(R,t)$ as a function of $R/\tilde{r}(t)$ is plotted in Fig. 6. What is not obvious from inspection of the figure is the fact that the total momentum inside the fluid is *strictly* zero (apart from exponentially small terms) for $t \gg \gamma^{-1}$ (this can be verified explicitly by summing up $R^2 Q_{\text{lgv}}(R,t)$ over R). Thus, the weak external positive momentum density exactly compensates the inner backflowing momentum. A second feature of this scaled spreading is that the (unscaled) momentum density $\tilde{r}(t)^{-3}(\gamma t)^{-1} Q_{\text{lgv}}(R,t)$ in the innermost region, where the asymptotic behavior $Q_{\text{lgv}}(R,t) \sim -[\tilde{r}(t)/R]$ is observable, is exactly equal to that of the conservative dynamics $\ell(t)^{-3} Q_{\text{melt}}(R,t)$; this is due to the fact that in that “aged” region, the local forces are dominated by the integro-differential term, that is, the viscoelastic term, and the influence of the friction becomes negligible. Notice that the

average momentum comprised inside this innermost region is $\propto -\mathbf{p}_0(\gamma t)^{-1}$.

Let us consider now the c.m. VAF of a tagged polymer chain as the average velocity of its c.m. after a perturbative instantaneous kick on each monomer of the chain [see Eq. (26)]. As in Secs. II B and II C the screening length $\tilde{r}(t)$ allows us to think of the tagged chain as being made of $N/g(t)$ subchains of length $g(t) \sim [\tilde{r}(t)/b]^2$. For each subchain one can consider that the $g(t)$ initial kicks have evolved enough to encompass all monomers within the asymptotic innermost region of the viscoelastic relaxation, where $Q_{\text{lgv}}(R, t) \sim [\tilde{r}(t)/R]$. As a result, each monomer of each subchain bears a typical momentum $-g(t)\mathbf{p}_0(\gamma t)^{-1}/n\tilde{r}(t)^3$. Thus, the c.m. VAF behaves as $\sim v_T^2 N^{-1}(\gamma t)^{-1}/[nb^2\tilde{r}(t)]$, which is the prediction (44) up to a numerical factor. This behavior can only be observed as long as $\tilde{r}(t) < R_g$. After a characteristic time $t^* \sim \bar{\gamma}^2 t_N$, defined by $\tilde{r}(t^*) \sim R_g$, the whole chain resides within a region of purely asymptotic viscoelastic relaxation where the friction term is no longer relevant (see above): As a consequence, the c.m. VAF returns to the γ -independent behavior Eq. (24), characteristic of momentum-conserving dynamics: $C_{\text{c.m.}}(t) \propto N^{-1/2}t^{-3/2}$ for $t^* \ll t \ll t_N$, in agreement with Eq. (46).

The results presented in this section are rederived in Sec. IV using the notion of a time-dependent Oseen tensor by probing the time-dependent mobility of a tagged polymer chain under a constant drag.

B. High versus low friction Langevin dynamics

The first regime of the c.m. VAF for a Langevin dynamics Eq. (44) relies on the parameter $\bar{\gamma}$, which is the ratio of the bare Langevin friction constant γm to the dressed monomeric friction constant ζ_1 . The preceding discussion showed how such a ratio emerges from a balance between a true microscopic dissipative mechanism (the Langevin friction) and a mesoscopic dissipative mechanism (the relaxation of internal Rouse modes). The typical value of the parameter $\bar{\gamma}$ strongly depends on the monomeric density n and the Langevin friction γ . For low values of the Langevin friction and rather dense melts, one expects $\bar{\gamma}$ to be small (for instance, typical values $\bar{\gamma} \sim 10^{-2}$ are obtained for the simulations presented in Ref. [11]) because W^{-1} is dominated by the cage effect which imposes large diffusion times fairly independent of small γ .

It is useful to discuss also the case where the Langevin friction γ is high with respect to what one would obtain for the monomer friction $\zeta_1^{(0)}/m = (\pi b^2 W^{(0)}/12)^{-1} v_T^2$ for the same system but with $\gamma = 0$ (recall that W depends on γ in a Langevin-driven system). In this case one expects that $\bar{\gamma}$ is not small; for diverging γ , $\bar{\gamma}$ should tend to a constant value (this can be understood by recalling that the reaction rate of an overdamped Brownian particle in a well is $\propto \gamma^{-1} \times$ Arrhenius factor [34]). The limiting value of $\bar{\gamma} = \bar{\gamma}_\infty$ depends on the density, with $\bar{\gamma}_\infty \lesssim 1$ for moderate densities.

The influence of $\bar{\gamma}$ on the c.m. dynamics is twofold. First, only small values of $\bar{\gamma}$ make it possible to observe a well-defined time window where the purely viscoelastic recovery regime, $C_{\text{c.m.}} \propto -t^{-3/2}/\sqrt{N}$, is observable. For high $\bar{\gamma} \sim 1$, this regime would mix with the crossover to the free diffusion (at the Rouse time). Second, it has a quantitative impact on

Eq. (44). For low values of $\bar{\gamma}$, we obtained $\xi(\bar{\gamma}) \simeq 0.1052/\sqrt{\bar{\gamma}}$ [see Eq. (45)] using the $\varphi \simeq 1$ approximation [see Eq. (17)]. This point highlights the fact that for $\bar{\gamma} \ll 1$, the VHI screening length $\tilde{r}(t) \sim \bar{\gamma}^{-1/2} b(Wt)^{1/4}$ is far larger than the diffusion blob size $r^*(t) \sim b(Wt)^{1/4}$: The length scales mainly responsible for the recovery behavior ($C_{\text{c.m.}} \propto -t^{-5/4}$) at a given time t can be considered as pertaining to a nonmoving polymer.

In the high friction limit $\bar{\gamma} \lesssim 1$, the relevant screening length $\tilde{r}(t)$ and the diffusion blob size $r^*(t) \sim b(Wt)^{1/4}$ are comparable, and the competing diffusion of the tagged polymer contributes to diminish the factor $\xi(\bar{\gamma})$ with respect to the asymptotic value for low $\bar{\gamma}$ [Eq. (45)]. Moreover, the same argument invalidates the hydrodynamic approximation, $E(k, t) \simeq E(t)$, for the shear modulus. Hence, we have to use a k -dependent expression for E . To stay at a rather qualitative level we introduce the following ansatz for $E(k, t)$ [inspired by a comparison of the general expression for $E(k, t)$, Eq. (A3), with the analogous expression for the form factor $F(k, t) = \sum_{i,j=1}^N \langle \exp[i\mathbf{k} \cdot (\mathbf{r}_j(t) - \mathbf{r}_i(0))] \rangle / N]$

$$E(k, t) \simeq E(0, t) \frac{F(k, t)}{F(k)} = E(t) \varphi(Ak^4 t), \quad (50)$$

which accounts roughly for the decay of the elastic response at a given length scale due to the diffusion of the chain blobs of comparable size.

Within this approximation, one can evaluate the effect of the blob diffusion on $C_{\text{c.m.}}(t)$. The resultant modification of the theory does not alter the formula Eq. (44), only the constant $\xi(\bar{\gamma})$ is modified to

$$\xi(\bar{\gamma}) = \frac{\bar{\gamma}^{-1}}{\sqrt{6\pi}^{5/4}} \int_0^\infty du u^{1/4} \varphi(u) J_{\bar{\gamma}}(u), \quad (51)$$

$$\widehat{J}_{\bar{\gamma}}(z) = \frac{\widehat{\beta}(z)^{-1}}{\widehat{\beta}(z)^{-1} + \bar{\gamma}^{-1}}, \quad (52)$$

$$\widehat{\beta}(z) = \frac{1}{\sqrt{\pi}} \int_0^\infty \frac{dy}{\sqrt{y}} \varphi(y) e^{-yz}. \quad (53)$$

The function $\xi(\bar{\gamma})$ and the comparison with the asymptotic behavior Eq. (45) are plotted in Fig. 7.

We see that the diffusion of the relevant blobs, when efficient, drives the response toward a weakening of the viscoelastic effect: The diffusion of the “elastic elements” and of the blobs of the tagged chain contributes to a partial blurring of the recovery effect. Also shown in the plot is the constant 0.037 representing the correlation hole effect [10].

As already mentioned, for high values of $\bar{\gamma}$, the dMCT and hMCT yield identical predictions for $C_{\text{c.m.}}(t)$, the sole difference being the prefactor. It is obvious from this figure that for moderate values of the friction, the viscoelastic relaxation mechanism remains largely dominant, the density-based contributions being negligible. This dominance is, however, dispelled at high friction, where both effects seem to be comparable. Such a situation is typically provided by Monte Carlo simulations where the effective friction is expected to be large. For the Monte Carlo dynamics, the dMCT or hMCT alone should be insufficient to account quantitatively for the $t^{-5/4}$ tail, and one should envisage mixing the two approaches together. The simplest way would be to add the

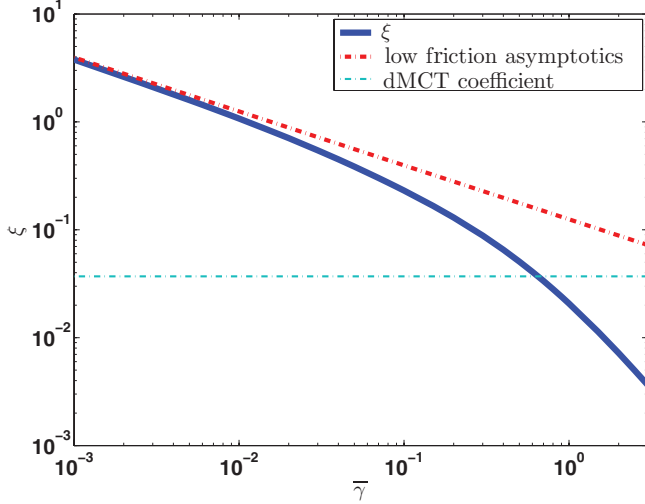


FIG. 7. (Color online) Prefactor ξ as a function of $\bar{\gamma}$. The solid line indicates the full theory including approximate wave-vector dependence of the shear modulus Eq. (51). The thick dash-dotted line shows the asymptotic behavior of ξ for small $\bar{\gamma}$ Eq. (45), and the thin dash-dotted line the constant value of ξ expected from the dMCT approach of Ref. [10].

two contributions [35], but the legitimacy of this ansatz is *a priori* questionable [23].

IV. GENERALIZED OSEEN TENSOR AND CHAIN MOBILITY

The anomalous diffusion effects considered in this paper physically hinge on the VHIs inherent in polymer systems. The VHIs can be expressed in terms of the generalized time-dependent Oseen tensor $\underline{\underline{\alpha}}(\mathbf{r}, t)$ defining the collective flow response, $\mathbf{v}(\mathbf{r}, t)$, to a perturbative external force with density $\mathbf{f}_{\text{ext}}(\mathbf{r})$ applied to the medium at $t > 0$ (the external force is zero for $t < 0$):

$$\mathbf{v}(\mathbf{r}, t) = \int \underline{\underline{\alpha}}(\mathbf{r} - \mathbf{r}', t) \cdot \mathbf{f}_{\text{ext}}(\mathbf{r}') d^3 r'. \quad (54)$$

An alternative approach, which complements the theory presented in the preceding sections, is to consider the response of the polymer c.m. to a constant drag force. The c.m. velocity response is closely related to the generalized Oseen tensor. From this Oseen tensor, which can be viewed as the resolvent of the generalized Navier-Stokes equation (27), we extract the isotropic part $\alpha(r, t) = \frac{1}{3} \text{Tr} \underline{\underline{\alpha}}(\mathbf{r}, t)$ (the Oseen response function), the truly important quantity for our purpose. One can show by the linear-response theory [21] that this function is related to the transverse current correlation function $C_T(k, t)$ by

$$C_T(k, t) = \frac{3}{2} n k_B T \frac{\partial \alpha(k, t)}{\partial t}. \quad (55)$$

In simple fluids and in the limit of large times, the Oseen function is well known [1,2]:

$$\alpha(r, \infty) = \frac{1}{6\pi \eta_s r}, \quad (56)$$

where η_s is the fluid viscosity. In the transient regime, that is, for finite t , the hydrodynamic interactions have a finite

range $\ell_s(t)$ characterized by the vorticity diffusion length $\ell_s(t) \sim \sqrt{t \eta_s / \rho_s}$, where ρ_s is the fluid mass density:

$$\alpha(r, t) \sim \begin{cases} \frac{1}{\eta_s r} & \text{if } r \lesssim \ell_s(t), \\ \text{exponentially small} & \text{if } r \gg \ell_s(t). \end{cases} \quad (57)$$

(Here and below we omit numerical factors for simplicity.) In the case of a simple fluid coupled to a Langevin thermostat, another screening length \tilde{r} is emerging [33], $\tilde{r} = \sqrt{\eta / \rho \gamma}$. In this case $\alpha(r, t) \sim 1/(\eta_s r)$ if $r \lesssim \ell_s(t)$ and $r \lesssim \tilde{r}$.

This simple qualitative picture can be easily generalized to account for viscoelastic effects in polymer melts. The only important difference is that there the stress relaxation is slow. Hence, the macroscopic viscosity η in the transient regime must be replaced by the effective transient viscosity $\eta(t) = \int_0^t dt' E(t')$: We have then $\eta(t) \sim k_B T n \sqrt{t} / \sqrt{W}$ in the t range between the monomer relaxation and the Rouse times, $t_1 \ll t \ll t_N$. The generalized viscoelastic (polymeric) Oseen response function therefore is

$$\alpha(r, t) \sim 1/(\eta(t)r), \quad r \lesssim \ell(t), \quad r \lesssim \tilde{r}(t), \quad (58)$$

where $\ell(t) \sim \sqrt{t \eta(t) / \rho}$ and $\tilde{r} = \sqrt{\eta(t) / \gamma \rho}$. While the rigorous justification of these inductive formulas comes from Eqs. (55) and (12), it is worth noticing here that (i) the $1/r$ dependence of $\alpha(r, t)$ comes from the gradient expansion of the viscous force $\propto \nabla^2 v$, which remains valid in the relevant regimes also for polymer melts; (ii) the validity of the replacement $\eta \rightsquigarrow \eta(t)$ is a direct consequence of the slow (power law) behavior of $E(t)$; (iii) as noticed in Sec. III, the Langevin screening length $\tilde{r}(t)$ is now time dependent.

This concept of generalized Oseen flow-to-force response function and VHI can be used to derive the main results of this paper (as presented in Ref. [11]). We suppose that a weak external force \mathbf{F} is applied to each unit of the tagged chain at $t > 0$. The general linear response of the c.m. velocity, $\mathbf{V}_{\text{c.m.}}(t)$, can be written as

$$\langle \mathbf{V}_{\text{c.m.}}(t) \rangle = \mathbf{F} \chi(t). \quad (59)$$

The FDT imposes a rigorous relation between the response function $\chi(t)$ and the c.m. velocity correlation function $C_{\text{c.m.}}(t)$:

$$C_{\text{c.m.}}(t) = \frac{k_B T}{N} \frac{\partial \chi(t)}{\partial t}. \quad (60)$$

The response function $\chi(t)$ has two main contributions: $\chi(t) = \chi_0(t) + \chi_h(t)$ coming from the Rouse velocity relative to the polymer matrix, $\chi_0(t) = 1/\zeta_1$, and the cooperative velocity $\mathbf{v}(\mathbf{r}, t)$ of the matrix induced by the external forces, $\chi_h(t) \mathbf{F} = \frac{1}{N} \sum_{i=1}^N \langle \mathbf{v}(\mathbf{r}_i, t) \rangle$, where \mathbf{r}_i denote the positions of tagged chain units. The first term χ_0 is constant and does not contribute to $C_{\text{c.m.}}(t)$. The cooperative term can be calculated using the generalized Oseen function:

$$\chi_h(t) = \frac{1}{N} \sum_{i,j} \alpha(r_{ij}, t) \sim \frac{1}{N \eta(t)} \sum_{i,j} \frac{1}{r_{ij}}, \quad (61)$$

where $r_{ij} = |\mathbf{r}_i - \mathbf{r}_j|$ and the second sum includes only such pairs (i, j) of tagged chain units that $r_{ij} \lesssim \ell(t)$ and $r_{ij} \lesssim \tilde{r}(t)$.

Equations (60) and (61) make it possible to easily get all the principal results for the c.m. VAF. Let us start with the momentum-conserving dynamics ($\gamma = 0$, $\tilde{r} = \infty$). If the

momentum diffusion length $\ell(t)$ exceeds the chain size, $\ell(t) \gtrsim R_g$, the $\widetilde{\Sigma}$ in Eq. (61) is constant ($\sim N^2/R_g$); hence, we get

$$C_{c.m.}(t) \sim \frac{k_B T}{R_g} \frac{\partial}{\partial t} \frac{1}{\eta(t)} \propto -N^{-1/2} t^{-3/2}, \quad t_N \gg t \gg \tau \quad (62)$$

in agreement with Eq. (24). Here the crossover time τ is defined by the condition $\ell(\tau) \sim R_g$ readily leading to $\tau \propto N^{2/3}$, in agreement with Eq. (21). The simple physical arguments outlined above thus explain all the main features of $C_{c.m.}(t)$ in this regime: The N dependence $C_{c.m.} \propto 1/\sqrt{N}$ (rather than $1/N$ as follows from the dmCT [10]) is defined by the chain size as $C_{c.m.} \propto 1/R_g$ and $R_g \propto \sqrt{N}$; the $t^{-3/2}$ power law comes directly from the time behavior of the transient viscosity, $\eta(t) \propto \sqrt{t}$; the sign of $C_{c.m.}$ is *negative* since $\eta(t)$ is *increasing* in time.

For shorter times, $t \ll \tau$, the diffusion length $\ell(t)$ is shorter than R_g ; hence, the $\widetilde{\Sigma}$ in Eq. (61) becomes time dependent,

$$\widetilde{\Sigma} \sim Ng(t)/\ell(t) \sim N\ell(t)/b^2, \quad (63)$$

leading to

$$C_{c.m.}(t) \sim \frac{1}{N} \frac{\partial}{\partial t} \frac{N\ell(t)}{N\eta(t)b^2} \propto N^{-1} t^{-3/4}, \quad t_1 \ll t \ll \tau. \quad (64)$$

The correlation function $C_{c.m.}(t)$ in this regime significantly depends on the visco-inertial diffusion length $\ell(t)$; $C_{c.m.} > 0$ since $\ell(t)$ is increasing faster than $\eta(t)$: $\ell(t) \propto t^{3/4}$, $\eta(t) \propto \sqrt{t}$.

The main results for the Langevin dynamics can be understood on the same footing. If γ is not too low, the Langevin screening length $\widetilde{r}(t)$ takes the control for $t \gg 1/\gamma$ [i.e., $\widetilde{r}(t) < \ell(t)$ in this time regime]. So the crossover time t^* between the two main dynamical regimes is defined by $\widetilde{r}(t^*) \sim R_g$; that is, $\eta(t^*)/(\rho\gamma) \sim Nb^2$ leading to $t^* \propto N^2\gamma^2$, in agreement with equations of Sec. III A. The screening is important for shorter times, $1/\gamma \ll t \ll t^*$, where $\widetilde{\Sigma} \sim N\widetilde{r}(t)/b^2$ [cf. Eq. (63)]; hence, for $\gamma^{-1} \ll t \ll t^*$ we have

$$C_{c.m.}(t) \sim \frac{1}{N} \frac{\partial}{\partial t} \frac{N\widetilde{r}(t)}{N\eta(t)b^2} \propto -N^{-1} t^{-5/4} \gamma^{-1/2}. \quad (65)$$

The $t^{-5/4}$ time behavior in this regime thus comes directly from $\widetilde{r}(t) \propto t^{1/4}$ and $\eta(t) \propto \sqrt{t}$ scaling laws. In addition, $C_{c.m.} \propto \gamma^{-1/2}$ following the similar dependence of the screening length. For long time, $t \gg t^*$, no screening is relevant, so we recover the behavior for $\gamma = 0$.

V. ON THE VALIDITY OF THE APPROACH

We are now in a position to summarize the main approximations involved in the theory. To this end, it is useful to have in mind the Oseen function (VHI)-based approach outlined above. Two assumptions were made. (i) We neglected monomer displacements (time dependence of r_{ij}) in Eq. (61). This is equivalent to neglecting the relaxation of the dynamical form factor $F(k, t)$, that is, to setting $F(k, t) = F(k)$. (ii) We neglected the wavelength dependence of the transient viscosity $\eta(t)$, that is, equivalently, disregarded a k dependence of the relaxation modulus $E(k, t)$.

Both assumptions can be justified in the same way. With the Rouse dynamics the typical monomer displacement during

time t is $r^*(t) \sim b(Wt)^{1/4}$. On the other hand, the characteristic length scale $k^{-1} \sim$ (“relevant” r_{ij}) is defined by one of three lengths: It is either the chain size R_g , or the diffusion length $\ell(t)$, or the Langevin screening length $\widetilde{r}(t)$. Obviously, $r^*(t) \ll R_g$ in the pre-Rouse regime. It can be also easily seen that $r^*(t) \ll \ell(t)$ for t beyond the monomer time t_1 [actually $r^*(t) \ll \ell(t)$ for any t since momentum diffusion is always much faster than monomer diffusion]. The two observations show that assumption (i) is always valid for $\gamma = 0$ since

$$k^{-1} \gg r^*(t). \quad (66)$$

The new characteristic length scale emerging with Langevin dynamics is $k^{-1} \sim \widetilde{r}(t) \sim \bar{\gamma}^{-1/2} r^*(t)$. Therefore, the condition Eq. (66) is valid as well if $\bar{\gamma} \equiv m\gamma/\zeta_1 \ll 1$. The validity of the assumption (ii) is ensured by the same condition (66) since one can easily see that $r^*(t)$ is simultaneously the typical size of an elastic element (chain fragment or dynamical blob) whose relaxation time is comparable to t . The condition (66) therefore says that the relevant elastic elements are much smaller than the characteristic length scale k^{-1} ; hence, the k dependence of $E(k, t)$ is indeed negligible.

The two effects disregarded by assumptions (i) and (ii) bring in a correction to the basic (asymptotically exact) result for the c.m. VAF. Our analysis of the Langevin dynamics (see Sec. III B) shows that the relative correction is negative and is proportional to $\sqrt{\bar{\gamma}}$ in the regime $1/\gamma < t < t^*$. The VHI correction term is therefore comparable with the density-fluctuation (dmCT) contribution (although the VHI correction has a larger magnitude and the opposite sign).

Let us now turn to a central assumption that has been hidden so far. Indeed, we assumed that the monomer displacement dynamics is Rouse-like, that is, is nearly not affected by the VHI effects. It can be easily justified. First, we use the FDT relation between the MSD of a monomer i on a tagged chain,

$$h(t) = \frac{1}{6} \langle [r_i(0) - r_i(t)]^2 \rangle, \quad (67)$$

and the velocity response to a weak force \mathbf{F} applied (at $t > 0$) to this monomer:

$$\langle v_i(t) \rangle = \frac{\mathbf{F}}{k_B T} \frac{\partial}{\partial t} h(t). \quad (68)$$

For $t \gg t_1$ the external force F induces a concerted motion of a relevant dynamical blob (chain fragment of g units with relaxation time $t_1 g^2 \sim t$). The blob Rouse friction constant is $g\zeta_1$, so the Rouse prediction is $\langle v_i(t) \rangle_0 \sim \frac{F}{g\zeta_1} \sim Wb^2 \frac{F}{k_B T} \sqrt{t_1/t}$. The cooperative flow (VHI) contribution is $\langle v_i(t) \rangle_h \sim \frac{F}{\eta(t)r_g} \sim \frac{W}{bn} \frac{F}{k_B T} (t_1/t)^{3/4}$, where $r_g \sim b\sqrt{g}$ is the blob size. Summing the two terms $\langle v_i(t) \rangle = \langle v_i(t) \rangle_0 + \langle v_i(t) \rangle_h$, using Eq. (68) and integrating, we get

$$h(t) \sim b^2 \sqrt{Wt} \left[1 + \frac{\text{const}}{nb^3} \left(\frac{t_1}{t} \right)^{1/4} \right],$$

where the second term in the square brackets represents the cooperative flow effect. This term is always small for $t \gg t_1$; hence, the VHI effect for the monomer diffusion is indeed negligible.

There is another subtle point associated with the one above, which we broached briefly in Sec. II C. In all the FDT reasonings we made throughout this paper, the external forces

were applied to volume elements while we considered them as acting on all monomers of a tagged chain. We therefore assumed that the external forces applied to the tagged chain were fully transferred to the surrounding matrix. This is a natural assumption because the tagged chain can be considered as a part of the matrix, and the chain fragments are strongly overlapping there, so the elastic forces due to the “deformed” tagged chain cannot provide but a minute contribution to the global elastic forces of the whole matrix.

All in all, the analysis presented above drives us to the conclusion that the theory developed in this paper yields asymptotically exact results in the declared parameter range (i.e., for $N \gg 1$, $t_1 \ll t \ll t_N$, $\bar{\gamma} \ll 1$).

VI. DISCUSSION AND CONCLUSIONS

In this paper, we showed that a relevant mode-coupling approach (referred to as “hMCT”) can be devised to study the c.m. diffusional properties of a tagged polymer in an unentangled melt. This approach is in accordance with a polymer-based theory presented in Ref. [11] and shows that in most cases the subdiffusional initial regime of the c.m. diffusion, not predicted by the Rouse theory, reflects transient VHIs in the melt: The motion of a tagged chain couples to the collective velocity field (hydrodynamic flow) of the melt, which diffuses due to the viscoelastic response of the melt. This VHI driven diffusion of momentum is used to calculate the c.m. VAF (Sec. II C) and c.m. MSD (Sec. II C4), leading to a rich relaxation behavior of the c.m. velocity [see, e.g., Eqs. (23) and (24); the simpler case of a diffusing polymer chain in a monomeric fluid is also analyzed in Sec. II B].

The physical picture outlined above is encapsulated in our “hydrodynamic MCT (hMCT)” approach where the “relevant decay channels” [36] are the collective (hydrodynamic) current fields. For momentum-conserving dynamics this mechanism is always dominant over the correlation hole effect [11], which was analyzed in part I through a dMCT assuming that the subdiffusive c.m. motion can be fully traced back to the coupling of the c.m. dynamics to the (collective and chain) density fluctuations of the melt [10].

The theoretical predictions of this paper are universal for long chains (of many Kuhn segments). Local interactions, such as bond-orientation potentials, merely renormalize the input parameters like the statistical segment and the monomer relaxation time. Although our theory was developed for unentangled melts, it is also relevant for the early time regime ($t < \tau_e$) of entangled polymer melts (Fig. 4). A more detailed comparison of the theory with simulations of different parameters, such as density, chain rigidity, or chain crossability, will be given elsewhere [37].

We also studied the case of non-momentum-conserving dynamics, widespread in numerical simulations where Monte Carlo or Langevin algorithms are often used to accelerate and stabilize the dynamics. In these cases, although the momentum diffusion seems to be less important, the hMCT is paradoxically still relevant, for it takes into account the slow decay of the viscoelastic relaxation of the melt. For small values of the Langevin friction and/or high densities (leading to low monomer mobility), we find the VHI effects to remain

the dominant mechanism (Sec. III). In the strong-friction and low-density regimes, however, we noticed in Sec. III B that the correlation hole effect gains in strength compared to the VHI effect and both mechanisms could have a comparable impact on the c.m. dynamics.

All the results obtained within the hMCT were physically interpreted along the lines of a linear response formalism, wherein the average response of a tagged polymer to an instantaneous force equally distributed over all monomers of the chain is directly proportional to the c.m. VAF by virtue of the FDT. In this way, we highlighted the complex relaxational dynamics of the c.m. driven by the viscoelastic response of the melt. In Sec. IV, a complementary approach was presented, also based on the linear response formalism, which emphasizes the VHI-mediated flow-to-force relation within the melt. The notion of a time-dependent Oseen tensor was introduced and discussed, and the results of the paper were recovered by computing the time-dependent mobility of the tagged chain under constant force. We showed that the actual notion of a “dynamical hydrodynamic screening” in melts is quite involved for observables addressing a delocalized object, like the c.m. of a tagged polymer.

Our conclusions about the importance of VHIs in polymer melts may seem to contradict the common view that hydrodynamic interactions are almost totally screened in concentrated polymer systems [2,38–42]. Noteworthy, this classical view comes from theories considering the solvent motion with respect to the polymer matrix which, however, is assumed to be immobile. This concept cannot be applied, not even formally, to polymer melts where there is no solvent. Hence, we took into account the polymer matrix flow and showed that it gives rise to important long-range viscoelastic hydrodynamic effects.

Our study also shows the ability of the MCTs to predict accurately the fluctuation dynamics of complex fluids in the liquid range, but at the same time, it highlights a crucial point: The choice of the relevant decay channels is of primary importance, and physical arguments must lead the way. This paper shows that this choice is not always obvious and sometimes can even be counterintuitive.

A relevant challenge would be to develop an MCT formulation which could account for viscoelastic effects and a connectivity signature in the dynamical structure factor starting from a microscopic basis, that is, without assuming (as we did in Ref. [10]) Rouse or dRPA expressions for $F(k, t)$ and $S(k, t)$. As a matter of fact, the MCT, more precisely the dMCT, has been extensively applied to the dynamics of supercooled regime, where its nonlinear structure predicts dynamical arrest in the vicinity of the MCT glass transition [36,43]. A natural perspective resulting from the present work would thus be to explore the relevance of the viscoelastic recovery in the supercooled regime of polymer melts.

ACKNOWLEDGMENTS

We thank O. Benzerara for managing the access to the HPC resources at the GENCI-IDRIS (Grant No. i2010091467), the “Pôle Matériaux et Nanostructure d’Alsace,” and the “Direction Informatique (Pôle HPC)” of the University of Strasbourg.

APPENDIX A: k -DEPENDENCE OF THE SHEAR RELAXATION MODULUS

In Eqs. (11) and (36) we assumed that the shear modulus $E(t)$ has its hydrodynamic (macroscopic) limiting value (for $k \rightarrow 0$) predicted by the classical Rouse model Eq. (13). Let us analyze this approximation. For pair potentials the exact expression of the microscopic stress tensor is given by Ref. [24]

$$\sigma_{xz}(\mathbf{k} = k\mathbf{e}_z) = \sum_i \left\{ -m v_{i,z} v_{i,x} + \frac{1}{2} \sum_{j \neq i} \frac{x_{ij}}{r_{ij}} \phi'(r_{ij}) \times \frac{1 - \exp(-ikz_{ij})}{ik} \right\} e^{ikz_i}, \quad (\text{A1})$$

where $x_{ij} = x_i - x_j$, $\mathbf{r}_{ij} = \mathbf{r}_i - \mathbf{r}_j$, and $\phi(r_{ij})$ is the interaction potential of particles i and j . If one keeps as usual only the dominant intrachain potential interactions $\phi(r_{i,i+1}) \simeq \frac{3k_B T}{2b^2} r_{i,i+1}^2$ [2] and considers only small k such that $kb \ll 1$, we can simplify the preceding expression to

$$\sigma_{xz}(\mathbf{k} = k\mathbf{e}_z) \simeq \frac{3k_B T}{b^2} \sum_a \sum_{j=1}^N z_{j(j+1)}^a x_{j(j+1)}^a e^{ikz_j^a}, \quad (\text{A2})$$

where a is the label of the a th polymer of the melt. The relaxation modulus is related to the stress correlation function by virtue of the FDT:

$$E(k, t) = (k_B T V)^{-1} \langle \sigma_{xz}(-k\mathbf{e}_z, 0) \sigma_{xz}(k\mathbf{e}_z, t) \rangle.$$

For uncorrelated chains the above expression transforms to

$$E(k, t) = \frac{9k_B T n}{N b^4} \left\langle \sum_{i,j=1}^N z_{i(i+1)}(0) z_{j(j+1)}(t) \times x_{i(i+1)}(0) x_{j(j+1)}(t) e^{ik[z_j(t) - z_i(0)]} \right\rangle. \quad (\text{A3})$$

Thus, we see that the relaxation modulus keeps a k dependence which follows the motion of monomers. As a result, we can neglect the k dependence in the relaxation modulus $E(k, t)$ provided that we consider, for a given t , modes with length scale k^{-1} significantly larger than the dynamical blob size $r^*(t) \sim b(Wt)^{1/4}$: $k^{-1} \gg r^*(t)$. This condition amounts to $Ak^4 t \ll 1$. [Note that $r^*(t)$ is the characteristic size of an elastic element (chain section) whose relaxation time $\sim t$.]

For the momentum-conserving dynamics, we have seen that the relevant scale k^{-1} in the short-time $t^{-3/4}$ regime is $\propto t^{3/4}$, whereas the relevant $k^{-1} \sim b\sqrt{N}$ in the second regime

($t \gg \tau$). It can be easily seen that in both cases the condition $k^{-1} \gg r^*(t)$ is always valid (in the range $t_1 \ll t \ll t_N$ between the monomer and the Rouse time). Therefore, in this case we can indeed neglect the space dispersion of E : the assumption $E(k, t) \simeq E(t)$ is fully justified. In a similar way it is easy to show that this assumption is also valid for non-momentum-conserving (Langevin) systems provided that $\bar{\gamma} \ll 1$.

APPENDIX B: c.m. VAF FOR LANGEVIN DYNAMICS—THE SIGN INVERSION BEHAVIOR

Here we consider $C_{c.m.}(t)$ for a polymer melt with Langevin thermostat in the regime of low Langevin friction $\bar{\gamma} = m\gamma/\zeta_1 \ll 1$. On the other hand, we assume that the Langevin friction is still significant [in particular, for the regime where $C_{c.m.}(t)$ changes sign], that is, that $\gamma\tau \gg 1$ [here τ , defined in Eq. (21), sets the sign-inversion time scale for the real momentum-conserving dynamics].

With Langevin friction the c.m. VAF sign inversion regime corresponds to $t \sim 1/\gamma$ and can be analyzed in a straightforward way using Eqs. (6), (36), and (37). The results are

$$\widehat{C}_{c.m.}(z) \simeq A' \frac{z^{1/4}}{(1+z/\gamma)^{1/2}}, \quad (\text{B1})$$

$$A' = \frac{2}{\pi} \frac{v_T}{b^2 N n} \left(\frac{\sqrt{2\pi W}}{\gamma} \right)^{1/2}. \quad (\text{B2})$$

The corresponding real-time c.m. VAF is

$$C_{c.m.}(t) \simeq A' \gamma^{5/4} f_\gamma(\gamma t), \quad (\text{B3})$$

$$t_1 \ll t \ll t^* \sim \bar{\gamma}^2 t_N, \quad (\text{B4})$$

$$1/\tau \ll \gamma \ll \zeta_1/m, \quad (\text{B5})$$

where

$$f_\gamma(y) = -\frac{1}{\pi\sqrt{2}} y^{-5/4} \int_0^\infty dy' \frac{|1-y'/y|^{1/2}}{1-y'/y} y'^{1/4} e^{-y'}. \quad (\text{B6})$$

The function $f_\gamma(y)$ shows the following asymptotic behavior:

$$f_\gamma(y) \simeq \frac{1}{\pi\sqrt{2}} \begin{cases} \Gamma(3/4) y^{-3/4}, & y \ll 1, \\ -\Gamma(5/4) y^{-5/4}, & y \gg 1. \end{cases} \quad (\text{B7})$$

Thus, for $\gamma t \ll 1$ the c.m. VAF follows Eq. (23) for the short-time momentum conserving dynamics, while for $\gamma t \gg 1$ the above equation agrees with Eq. (44). The sign-reversal time is $t_0 \approx 0.78/\gamma$; that is, it is defined solely by the Langevin friction in this regime.

-
- [1] P. de Gennes, *Scaling Concepts in Polymer Physics* (Cornell University Press, Ithaca, NY, 1979).
 [2] M. Doi and S. F. Edwards, *The Theory of Polymer Dynamics* (Oxford Science, Oxford, 1989).
 [3] W. Paul and G. D. Smith, *Rep. Prog. Phys.* **67**, 1117 (2004).
 [4] G. D. Smith, W. Paul, M. Monkenbusch, and D. Richter, *Chem. Phys.* **261**, 61 (2000).
 [5] W. Paul, *Chem. Phys.* **284**, 59 (2002).

- [6] A. Kopf, B. Dünweg, and W. Paul, *J. Chem. Phys.* **107**, 6945 (1997).
 [7] W. Paul, G. D. Smith, D. Y. Yoon, B. Farago, S. Rathgeber, A. Zirkel, L. Willner, and D. Richter, *Phys. Rev. Lett.* **80**, 2346 (1998).
 [8] K. Kremer and G. S. Grest, *J. Chem. Phys.* **92**, 5057 (1990).
 [9] W. Paul, K. Binder, D. W. Heermann, and K. Kremer, *J. Chem. Phys.* **95**, 7726 (1991).

- [10] J. Farago, A. N. Semenov, H. Meyer, J. Wittmer, A. Johner, and J. Baschnagel, preceding paper (part I). *Phys. Rev. E* **85**, 051806 (2012), the preceding paper.
- [11] J. Farago, H. Meyer, and A. N. Semenov, *Phys. Rev. Lett.* **107**, 178301 (2011).
- [12] J. Farago, H. Meyer, J. Baschnagel, and A. N. Semenov, *J. Phys.: Condens. Matter* (in press).
- [13] J. P. Wittmer, P. Polinska, H. Meyer, J. Farago, A. Johner, J. Baschnagel, and A. Cavallo, *J. Chem. Phys.* **134**, 234901 (2011).
- [14] J. P. Boon and S. Yip, *Molecular Hydrodynamics* (Dover, Mineola, NY, 1992).
- [15] H. Sigurgeisson and D. M. Heyes, *Mol. Phys.* **101**, 469 (2003).
- [16] B. J. Alder and T. E. Wainwright, *Phys. Rev. Lett.* **18**, 988 (1967).
- [17] J. R. Dorfman and E. G. D. Cohen, *Phys. Rev. Lett.* **25**, 1257 (1970).
- [18] J. J. Erpenbeck and W. W. Wood, *Phys. Rev. A* **32**, 412 (1985).
- [19] D. Levesque and W. T. Ashurst, *Phys. Rev. Lett.* **33**, 277 (1974).
- [20] M. A. van der Hoef and D. Frenkel, *Phys. Rev. A* **41**, 4277 (1990).
- [21] J. P. Hansen and I. R. McDonalds, *Theory of Simple Liquids*, 3rd ed. (Academic Press, San Diego, 2006).
- [22] T. Gaskell and S. Miller, *J. Phys. C* **11**, 3749 (1978).
- [23] L. Sjogren and A. Sjolander, *J. Phys. C* **12**, 4369 (1979).
- [24] U. Balucani and M. Zoppi, *Dynamics of the Liquid State* (Oxford University Press, Oxford, 1995).
- [25] B. H. Zimm, *J. Chem. Phys.* **24**, 269 (1956).
- [26] V. Lisy, J. Tothova, and A. V. Zatorovsky, *J. Stat. Mech.: Theory Exp.* (2008) P01024.
- [27] D. Chandler, *Introduction to Modern Statistical Mechanics* (Oxford University Press, Oxford, 1987).
- [28] Why we can use safely in this case the true hydrodynamic limit $E(t) = E(k = 0, t)$ of the shear modulus, which in principle depends on k , is explained in Sec. III.
- [29] T. Soddemann, B. Dünweg, and K. Kremer, *Phys. Rev. E* **68**, 046702 (2003).
- [30] M. Rubinstein and R. H. Colby, *Polymer Physics* (Oxford University Press, Oxford, 2003).
- [31] Note that the transverse current correlation function $C_T(k, t)$ is equal to $\frac{3}{2}v_T^2$ times the 3d-Fourier transform of $Q_{\text{melt}}(R, t)\ell(t)^{-3}$.
- [32] R. B. Bird, R. C. Armstrong, and O. Hassager, *Dynamics of Polymeric Liquids: Fluid Mechanics*, Vol. 1 (Wiley, New York, 1987).
- [33] B. Dünweg, *J. Chem. Phys.* **99**, 6977 (1993).
- [34] N. G. Van Kampen, *Stochastic Processes in Physics and Chemistry* (North-Holland, Amsterdam, 2007).
- [35] S. A. Egorov, *J. Chem. Phys.* **134**, 084903 (2011).
- [36] W. Götze, *Complex Dynamics of Glass-Forming Liquids* (Oxford Science, Oxford, 2009).
- [37] H. Meyer, J. Farago, A. N. Semenov *et al.* (unpublished).
- [38] K. F. Freed and S. F. Edwards, *J. Chem. Phys.* **61**, 3626 (1974).
- [39] P. G. de Gennes, *Macromolecules* **9**, 594 (1976).
- [40] S. F. Edwards and M. Muthukumar, *Macromolecules* **17**, 586 (1984).
- [41] G. H. Fredrickson and E. Helfand, *J. Chem. Phys.* **93**, 2048 (1990).
- [42] P. Ahlrichs, R. Everaers, and B. Dünweg, *Phys. Rev. E* **64**, 040501 (2001).
- [43] S.-H. Chong and M. Fuchs, *Phys. Rev. Lett.* **88**, 185702 (2002).